Modeling of Pneumatic Tires by a Finite Element Model for the Development a Tire Friction Remote Sensor

H. Hölscher [1], M. Tewes, N. Botkin, M. Löhndorf, K.-H. Hoffmann, and E. Quandt

Center of Advanced European Studies and Research (caesar), Ludwig-Erhard-Allee 2, 53175 Bonn, Germany

Abstract

The behavior a pneumatic tire is analyzed and simulated using a finite element model. We calculate the elastic deformations in the contact area of a pneumatic tire touching the street for different friction conditions between tire and street. The simulations are compared with the experimental results. The comparison demonstrates that the overall deformation as well as the frictional behavior in the tire/ground contact area can be successfully simulated by finite element models.

Key words: Intelligent tire, remote passive sensor, tire simulation, tire friction

1 Introduction

Today, nearly all ground vehicles use wheels. These wheels have to support the weight of the vehicle, cushion the vehicle over surface irregularities, provide sufficient traction for driving and braking, and provide steering control and direction stability. Pneumatic tires can perform these functions effectively and efficiently. Consequently, they are universally used in today's road and off-road vehicles [1].

In order to enhance the performance of cars with pneumatic tires different approaches were applied to include a sensor into the rubber of the tire measuring the deformation and forces that occur in the tire/ground contact area [2–8].

[1] Now at: Center for NanoTechnology, University of Münster, Gievenbecker Weg 11, 48149 Münster, Germany

This information can be used for for the registration of the so-called "slip position", which indicates the loss of gripping power even before the tire begins to slip. As a consequence such a sensor can be implemented for the development of new tires with improved force transmission at different driving conditions as well as in the development of improved an *antilock braking system* (ABS) and/or *electronic stability program* (ESP) increasing the active vehicle safety. Furthermore, the proposed system might also be able to detect critical conditions of the tire itself like insufficient pressure or overheating. Consequently, such an *intelligent tire* prevents tire explosion and reduces maintenance costs and environmental impact by increasing the tire's lifetime.

During the last years, several concepts of tire sensors have been reported (see, e.g., [2–8] and references therein). A well established concept is the so-called *Darmstädter Tire Sensor*. It is able to detect the deformation of single tread elements in the tire road contact area in x-, y- and z-direction. The sensor measures the motion of a magnet relative to hall generators which are either attached to the tire at the inner side of the belt (kevlar belt tires) or placed within a single tread element (standard steel tires). The magnet is always placed in the tread rubber. The forces acting in the contact patch have been investigated on test stands and with specially prepared cars (see, e.g., Refs. [2–4]).

Another tire sensor system is the *sidewall torsion sensor* (SWT) [5] developed by Continental AG, Germany. This system is based on the measurement of the deformation in the sidewall of a pneumatic tire. The SWT system consists of a magnetized tire, wheel module with magnetic field sensors and signal processing and a central processing unit. The magnetic field of the magnetized tire is picked by the magneto-resistive sensor that is mounted on the wheel suspension. The sidewall stiffness depends on the inflation pressure and the lateral force acting in the contact patch. It has been demonstrated by the manufacturer that the sidewall torsion sensor can be used to enhance the overall behavior of a car.

Recently, we reported on our tire friction remote sensor [8]. To gain a broad acceptance of a tire remote sensor such a system has to meet the general specifications of the automotive industry. Especially, the transmission of the rapid changing force and strain data from the rotating tire is a challenge. The required data rate of some kHz for the improvement of ABS and/or EPS exceeds that of commercial available remote tire pressure measurement systems by a million. Therefore, the power consumption of an active transponder system would exceed by far the energy a battery could provide over the tire's lifetime. For that reason our development was focused on the remote readout of resonant circuits. This approach requires no power supply for the sensor itself and allows a high data transmission rate.

The basic principle of the currently developed remote tire sensor is shown in Fig. 1. The sensor is mounted into the tread of the pneumatic tire. The physical properties measured by the sensor (friction, load, tire pressure, ...) are submitted as radio frequency signals which are detected by a receiver. Subsequently, they can be used as an input to electronic controls like ABS or ESP. The concept of the sensor itself is based on a LC-tag. In this way, the measurement signal is encoded in a detuning of the resonant circuit. The sensor itself is sensitive to strain or stress.

Here we report about the supporting analysis and simulation of pneumatic tires for the development of the tire sensor. The behavior of a pneumatic tire is analyzed and simulated with a *finite element model* (FEM). Using this approach it is possible to calculate the elastic deformations in the contact area of a pneumatic tire touching the street. This is especially valuable because many quantities can be only measured with high experimental efforts at real tires. Therefore, the numerical simulation reduces costs and time for the development of the tire sensor. The simulations are compared with the experimental results obtained with different types of sensors. The comparison demonstrates that the overall deformation as well as the frictional behavior in the tire/ground contact area can be successfully simulated by finite element models.

2 Modeling and Simulation of Pneumatic Tires

2.1 Constraints to be considered

Modern pneumatic tires consist of a specific combination of rubber compounds, cord and steel belts (see Fig. 2). The main parts of a modern pneumatic tire are its body, sidewalls, beads, and tread. The body is made of layers of rubberized fabric, called plies, that give the tire strength and flexibility. The fabric is made of rayon, nylon, or polyester cord. Covering the plies are sidewalls and tread of chemically treated rubber. The sidewalls form the outer walls of the tire. Embedded in the two inner edges of the tire are steel loops, called beads, that hold the tire to the wheel. In a modern tubeless tire the seal between the beads and the wheel rim is airtight and the underside of the tire body is coated with butyl rubber to keep the air from escaping. The rubber components have different characteristics in dependence of their functionality. The tread for example gets in direct contact with the ground and has to be much harder than the sidewall.

When a driving torque is applied to a pneumatic tire, a tractive force is developed at the tire-ground patch [1]. Consequently, the tread before and in the contact area is compressed and a shear deformation of the sidewall of the tire is developed. As the tread is compressed before entering the contact region, the distance that the tire travels when subject to a driving torque will be less than that in the free rolling case. This phenomenon is the so-called longitudinal *slip* which is usually defined as

$$slip = \left(1 - \frac{r_{eff}}{r_{free}}\right) \times 100\% \tag{1}$$

where r_{eff} is the effective radius and r_{free} the radius of the free rolling tire [1].

When a driving torque is applied, the tire rotates without the equivalent translatory progress and a slip results. If the tire is rotating at a certain angular speed but the linear speed of the tire center is zero, then the longitudinal slip of the tire will be 100%. A situation often observed on icy surfaces.

2.2 Simulation of a Tire by a Finite Element Model

The above constraints had to be considered for the simulation of a pneumatic tire by the finite element model. The software packages MSC.MENTAT and MSC.MARC were used for the set-up and the calculation of the model, respectively. The results were subsequently analyzed by self-developed software routines. The set-up of the finite element model is based on the model of Tönük *et al.* [9,10]. Mainly the reinforcement by cord and steel have been changed due to a different software version of MSC.MARC. The simulation procedure includes the following features:

specific behavior of rubber: (*Mooney* material) Like many other polymer material vulcanized rubber shows a nonlinear stress-strain relationship. Furthermore, rubber is incompressible. This behavior is well described by the Mooney-Rivlin material formulation which is included in the MSC.MARC program.

constant inflation pressure: In a tire, the inflation pressure acts perpendicular to its inner surface. This effect is well described by the follower force option of MSC.MARC: A constant surface force is added to every element at the inner surface of the tire and the direction of this force is kept perpendicular to the surface during each solution increment. In a real inflated tire, the amount of air is fixed. Therefore, the pressure increases slightly if the tire is deformed. This small effect is ignored.

reinforcement by cord and steel: The reinforcement of the tire structure is very important for the overall behavior of pneumatic tires used today. The cord and steel plies have a well defined orientation and thickness. They are modeled by rebar elements which are superimposed to elements describing the matrix rubber elements (this feature is included in MSC.MARC, other finite element codes use different methods). The rebar elements stabilize the tire and follow all deformations of the rubber elements. [2]

tire/rim contact: The contact of the tire to the rim is simplified with the assumption that the tire sticks at the rim. The nodes at the tire/rim contact are fixed at the rim with the glue option of the MSC.MARC program. The bead bundle, which keeps the tire on the rim and supplies a stiff support of the body ply is ignored.

Coulomb friction at tire/street contact: The ground contact of the tire complicates the finite element model, since contact and friction problems are highly nonlinear. Nonetheless, both effects cannot be ignored. The contact problem in the FEM model is described by a deformable body (tire) to a rigid body (street) option. The Coulomb friction is modeled by the algorithm in MSC.MARC, which considers static and sliding friction between the nodes of the tire and the street modeled a smooth plane. The friction coefficient is different if the velocity between two bodies is zero (static friction) or nonzero (sliding friction). This behavior is modeled by an algorithm implemented in MSC.MARC.

tire rotation and slip: The tire rotation is performed by a discrete rotation of the rim for each increment. Since the tire is fixed to the rim it rotates and is deformed due to friction in the contact area. The slip between tire and street was controlled by the simultaneous movement of the street, i.e., for a slip of 90% the optimal street movement was reduced by 10%.

symmetry: In the current stage of the remote tire sensor project, the analysis of tire is simplified and it is assumed that the tire rolls straightforward along the roadway. In this case there are no additional lateral (cornering) forces. Therefore, the simple symmetry of the tire is used and only one half of the pneumatic tire is modeled by the finite element model (s. Fig. 3). The nodes at the symmetry plane were perpendicularly fixed to it (along the z-direction).

Figure 3 shows an overview of the described FEM model. The described components and materials are shown by different colors. The major numerical difficulties are the geometric non-linearities due to large deformations, the incompressibility of elastomers, and the specific boundary conditions of the tire/street contact. These effects consume the main computer time.

The parameters chosen for the finite element model correspond to a typical 195/65 R 15 tire. Consequently, the simulations provide information over the

[2] In difference to Refs. [9,10] we did not use a specific user routine to determine the actual orientation of the matrix rebar element. We found that this is not necessary in the used MSC.MARC 2000 Version and applied successfully the included rebar orientation option.

parameters	used values			
dimensions	195/65 R15 tire			
Mooney constants	C_{10}	C_{01}		
bead filler	14.14 MPa	21.26 MPa		
sidewall	171.8 kPa	830.3 kPa		
undertread	140.4 kPa	427 kPa		
tread	806.1 kPa	1.805 MPa		
reinforcement	n	A	E	ν
steel belts (±20°)	1000/m	0.3 mm^2	200 GPa	0.3
cord ply	1000/m	0.28 mm^2	3.97 GPa	0.3

Table 1
Summary of the parameters used in the finite element model.

overall behavior of a tire with these dimensions. The specific values of the used parameters are summarized in Fig. 1. The Mooney constants of the used rubber components are values given in Ref. [10]. The parameters used for the rebar elements in the simulation are typical values for modern pneumatic tires [10,12].

Depending on the requested accuracy the size of the elements is adapted and the number of elements is chosen between 5 000 and 20 000. Since the tire is strongly deformed in the contact area between tire and pavement, more elements must be used in this region. To obtain a finer grid in the contact areas the tire is splitted into sectors with elements of different size and angle. The sector getting in contact with the street contains elements covering 0.5° of the tire circle. This angle is increased to 5° in the sector opposite to the contact region, since this part of the tire is only slightly deformed. We verified that a finer grid does not change the outcome of the simulations. All data shown in the next sections was obtained with 17 496 elements (including the rebar elements).

The complete simulation procedure includes three simulation steps. First, the tire was inflated to a pressure between 2 and 3 bar. In a second step the tire is pressed on a flat plane modeling the contact with a real pavement. Typical applied normal loads range from 2000 N to 4000 N. Finally, the tire rotates and rolls over the street, where we considered different friction coefficients and slip values.

3 Comparison with Experimental Results

3.1 Loading of the Tire

In order verify the parameters of the finite element model we compared the loading of the tire in the simulation with experimental data. Figure 5 displays the load vs. deflection behavior of a Goodyear GT2 195/65 R 15 pneumatic tire measured on a tire sensor test rig at `caesar` (see Fig. 4). The colored symbols with errorbars represent three different measurements done with a tire pressure of 2.0, 2.5 and 3.0 bar. As it can be expected the deformation of the tire increases non-lineary with load and depends on the inflation pressure, i.e., lower deflection for higher inflation and vice versa.

The simulated deflection curves are plotted by three colored lines for different tire pressures in Fig. 5. The overall behavior is quite comparable. Remembering that the finite element model describes a "typical" tire – and not the specific properties of the GT2 tire – the agreement is remarkable and supports the reliability of the finite element model.

3.2 Tire Curvature (π-Sensor)

A sensor detecting the curvature of the tire was firstly integrated into a pneumatic tire in order to check the transmission of the sensor signals by the receiver. A second motivation for these measurements was the idea to use such a sensor as a tool to determine the actual tire pressure and loading through the measurement of the tire curvature. Due to the measurement principle this type of sensor was named π-sensor. Figure 6a) shows the basic idea. With increasing load the tire deforms mainly in the contact patch. By measuring the resulting tire shape it should be possible to determine the actual loading for a given tire pressure.

This idea is verified by the results of the finite element model. Calculating the tire shape for different loads and pressures we found that there is a unique relationship between tire shape and these boundary conditions. Figure 6b) displays the tire shape for different conditions. It is flat in the contact zone and the width of this contact zone increases with load and decreases with pressure.

From these shape curves we calculated the corresponding curvature curves as a function of the x-direction (see Fig. 7a). The curvature increases shortly before and after the contact zone and is almost zero in the contact patch. This behavior can be expected since the tire is flat in the contact zone. The corresponding experimental results show reasonable agreement with the simulation.

In Fig. 7b), the experimentally obtained curvature curves are plotted as a function of position along the traveling path of a real tire. They show the same overall behavior as the theoretical curves. The results shows that the width and the height of curvature curve depend on pressure and loading. This enables the π-sensor to detect, if pressure is correct for the actual loading. The analysis of experimental results show that the tire pressure can be measured with an accuracy of 0.1 bar which is a reliable value for many practical reasons.

3.3 Stress and Strain in the Contact Area (Friction Sensor)

Future sensor systems have to detect not only the tire loading and pressure. but also the actual street conditions like icy roads. Therefore, our work focused on the influence of different friction coefficients on the deformation of a pneumatic tire. In order measure the forces acting laterally to the contact patch, the simulations now analyze the stress and strain along the traveling path of the wheel.

The basic effects of different friction conditions on the deformation of the contact patch is described by the theory of Julien reviewed in Ref. [1]. The contact patch is divided into two regions. In the *adhesion region* the rubber is deformed but there is no sliding between the tire tread and the street. This region is in the front of the contact patch. The *sliding region*, however, is in the end of the contact patch. Here the tractive forces are so large that the rubber tread slides over the street.

In order to analyse the basic features of a wheel/street contact for different friction coefficient we begun our simulations with a simplified two-dimensional tire model. This model consists of a fixed rim covered with solid rubber ($E = 14\,\mathrm{MPa}$ and $\mu = 0.5$). Calculating the stress along the x-direction we obtained different curves in dependence on the actual friction conditions. As shown in Fig. 8a) this behavior is most prominent in the back area of the contact patch, where the maximum of the longitudinal stress increases with the friction coefficient. However, it is important to mention that even without any friction ($\mu = 0.0$) the stress is not constant along the x-direction. This effect superimposes the stress caused by friction and results from the simultaneous loading of the tire. Nonetheless, the result demonstrates that friction has indeed an influence on the deformation of a pneumatic tire. Consequently, this effect can be used as an indicator for the actual road conditions.

The stress in the contact patch changes also with slip. This is shown in Fig. 8b). With increasing slip the minimum of the curves shifts to the left and increases. Furthermore the area where the frictional forces between tire and road are given by static friction decreases. This is shown in both graphs by thick lines marking the adhesion region. This part of the curves is identified by the Coulomb friction mechanism implemented in MSC.MARC, i.e., the nodes of the finite element model are divided into nodes which are in a static or sliding friction state. It can be observed that the complete contact patch is in the sliding regime for a slip of 20 %, i.e., tire and street slide against each other.

Comparable results are obtained with the three-dimensional tire model. The stress and strain in the contact patch are shown in Fig. 9 for different street and slip conditions. As in the two-dimensional model the deformation of the tire is superimposed by its loading, but the expected effect – different deformation for different road conditions – is clearly observed.

Stress and strain change with the actual friction coefficient μ. The minima and maxima of the curves change there positions and absolute values in dependence of the street conditions. The overall behavior of the strain curves is comparable to the results found with the Darmstädter Tire Sensor [2]. The absolute differences of the curves are more pronounced in the strain curve. This effect is caused by the nonlinear stress-strain relationship of the rubber (Mooney-material).

Furthermore, the stress and strain curves change with the actual slip value. This is shown by the red dashed line for the friction coefficient of 0.5. There is a remarkable change of the stress and strain curve, if the slip is increased from 0 to 5 %.

4 Summary

To summarize, the presented finite element model is able describe the overall behavior of a real pneumatic tire. Experimental results could be confirmed by the simulations. The load vs. deflection relationship and the curvature curves (π-sensor) measured with the test facilities at `caesar` are in agreement with the finite element model. The calculation of stress and strain in the contact area verified that the deformation of the tire provide information about the actual road (μ-value) and driving (slip) conditions.

Acknowledgment

It is a pleasure to acknowledge helpful discussions about this project with C. Boes, R. Zimmerer (Goodyear, Luxemburg) and U. Gleu (Technical University, Berlin, Germany). Furthermore, we thank E. Tönük (Middle East Technical University, Ankara, Turkey) for sending us a copy of his Ph. D. Thesis. This work was supported by the EU via BMBF project 03N30089 (EUREKA project !2375: Tyre friction remote sensor using giant magneto-impendance).

References

[1] J. Y. Wong: *Theory of Ground Vehicles*, 3rd ed., Wiley-Interscience (2001).

[2] D. Ludwig, Ph. D. Thesis, Technische Universität Darmstadt (1997).

[3] Th. Bachmann, Ph. D. Thesis, Technische Universität Darmstadt (1997).

[4] M. Fach, V. Bachmann, B. Breuer: *Der Darmstädter Reifensensor im Labor und am Fahrzeug* in *2. Darmstädter Reifenkolloquium*, B. Breuer (Ed.),VDI Fortschrittsberichte Nr. 362 (1998).

[5] Th. Becherer: *The Sidewall Torsion Sensor System*, in *2. Darmstädter Reifenkolloquium*, B. Breuer (Ed.), VDI Fortschrittsberichte Nr. 362 (1998).

[6] A. Pohl, R. Steindl, L. Reindl, IEEE Trans. on Instr. Meas. **48**, 1041 (1999).

[7] O. Yilmazoglu, M. Brandt, J. Sigmund, E. Genc, H. L. Hartnagel, Sensor and Actuators **94**, 59 (2001).

[8] M. Tewes, M. Löhndorf, A. Ludwig, E. Quandt, Technisches Messen **68**, 292 (2002).

[9] E. Tönük, Ph. D. Thesis, Middle East Technical University, Ankara, Turkey (1998)

[10] E. Tönük, Y. S. Ünlüsoy, Comput. Struct. **79**, 1219 (2001).

[11] MSC.MARC Handbook (2000).

[12] U. Gleu, Ph. D. Thesis, Technische Universität Berlin (2000).

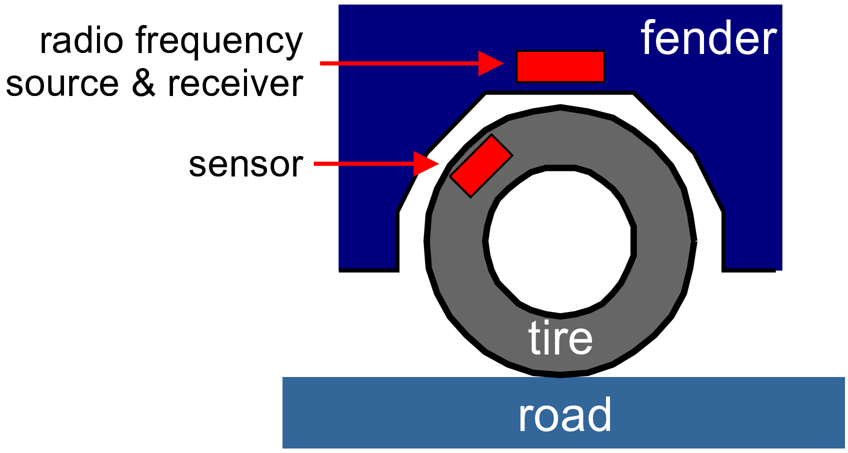

Fig. 1. The basic concept of the tire sensor detecting physical properties like tire pressure, temperature, friction, and loading. Its signals are send to a receiver and analyzed by further electronics in the car.

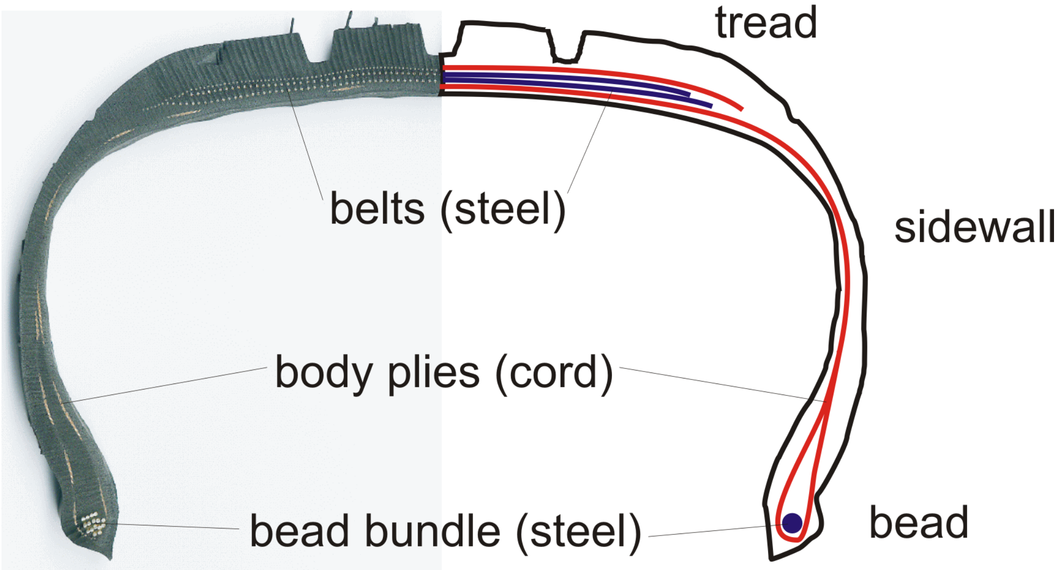

Fig. 2. Schematic of a modenr tire construction. The left photo shows a cut trough a todays pneumatic tire. The schematic on the right discribes the most important parts considered by the finite element model.

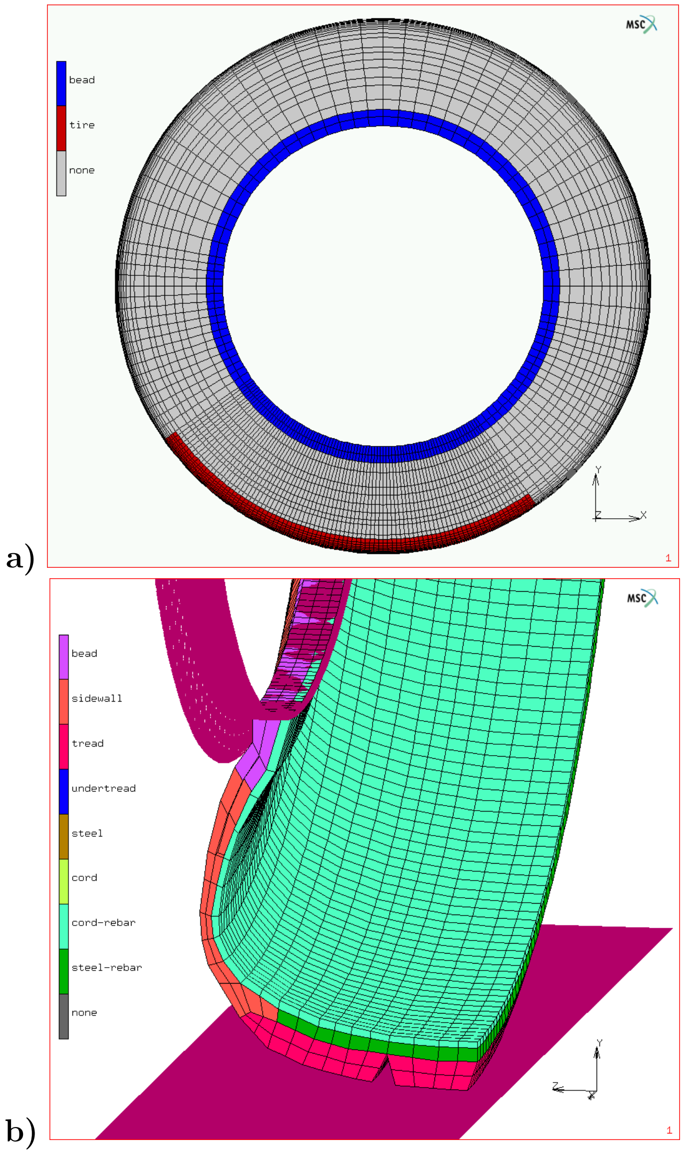

Fig. 3. **a)** Sideview of the tire. **b)** Cut through the finite element model. The different materials can be identified by colors.

Fig. 4. The tire test rig at allows measurement with $\approx 70\,\mathrm{km/h}$ and a loading up to 3700 N.

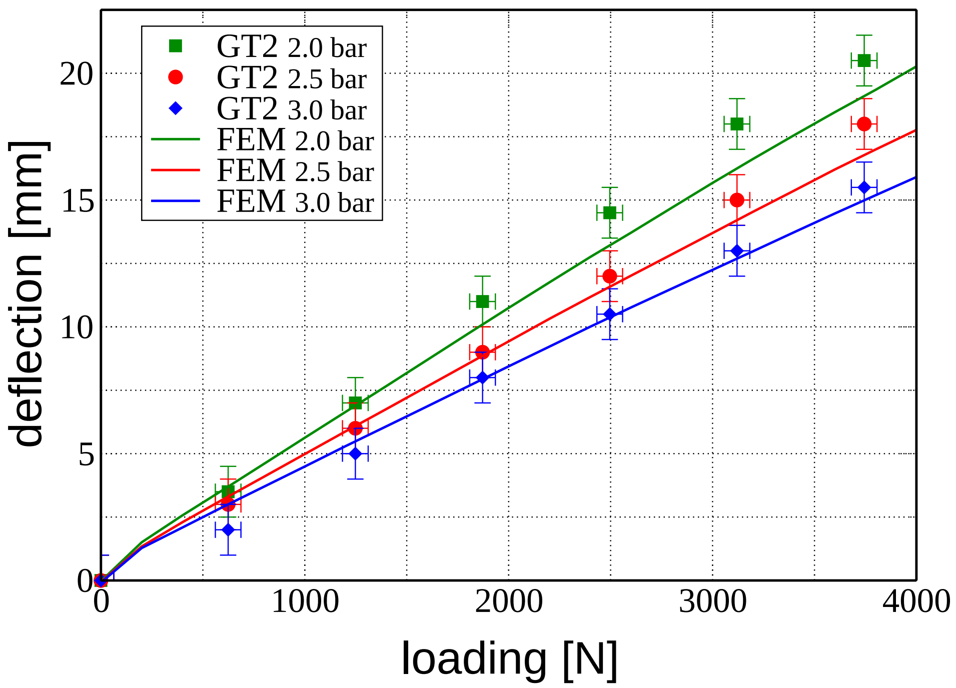

Fig. 5. The load vs. deflection behavior of the GT2 tire in dependence of the tire pressure. The symbols and lines show experimental and FEM results, respectively.

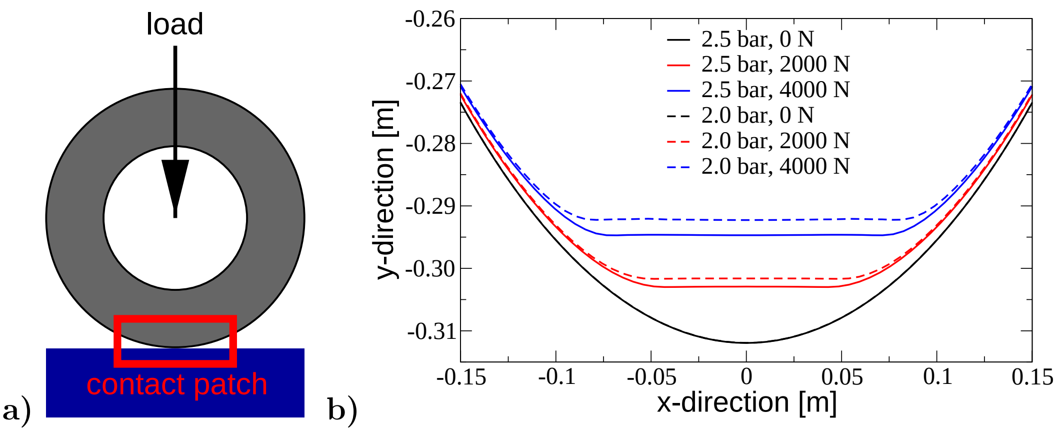

Fig. 6. **a)** Illustration of the basic idea of the π-sensor. **b)** The shape of the tire as calculated with the finite element model for different loads and pressures.

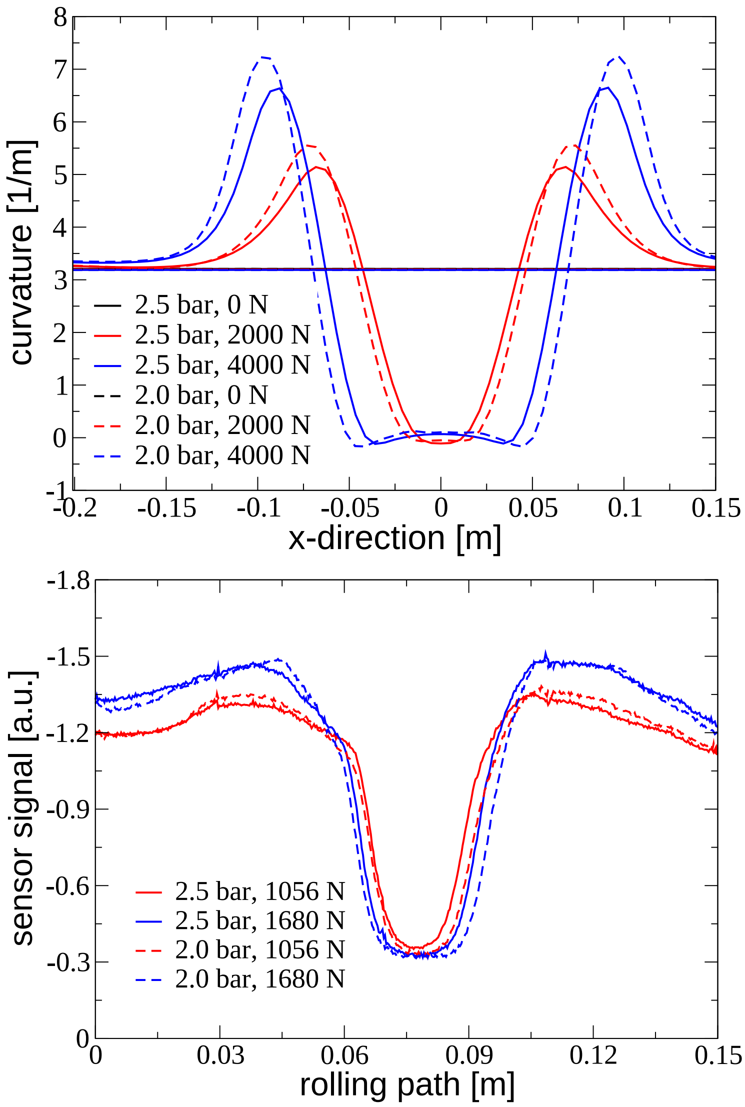

a)

b)

Fig. 7. **a)** The curvature curves calculated from the simulated data shown in Fig. 6b). **b)** The curvature curves measured with the π-sensor on the test rig.

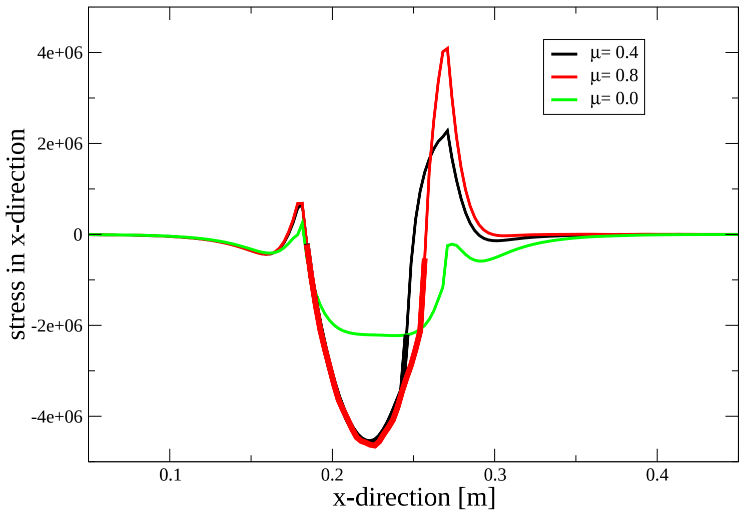

a)

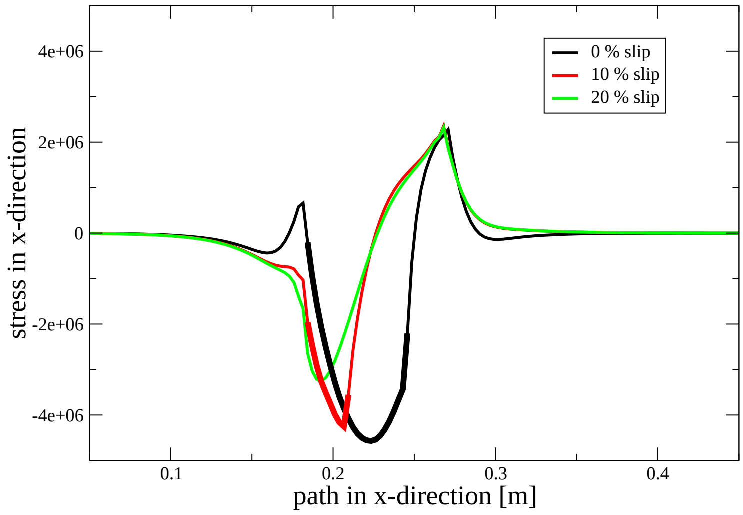

b)

Fig. 8. **a)** Stress in x-direction at the simple 2D-model without slip. The curves show the result for different road conditions (μ-values). The thick lines mark sticking nodes, i.e., the static friction area. **b)** Stress curves for different slip conditions. The friction coefficient was assumed to be $\mu = 0.4$.

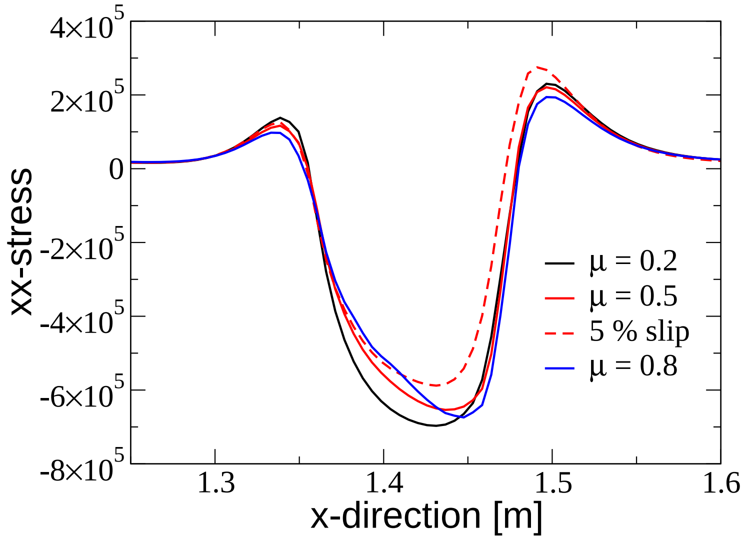

a)

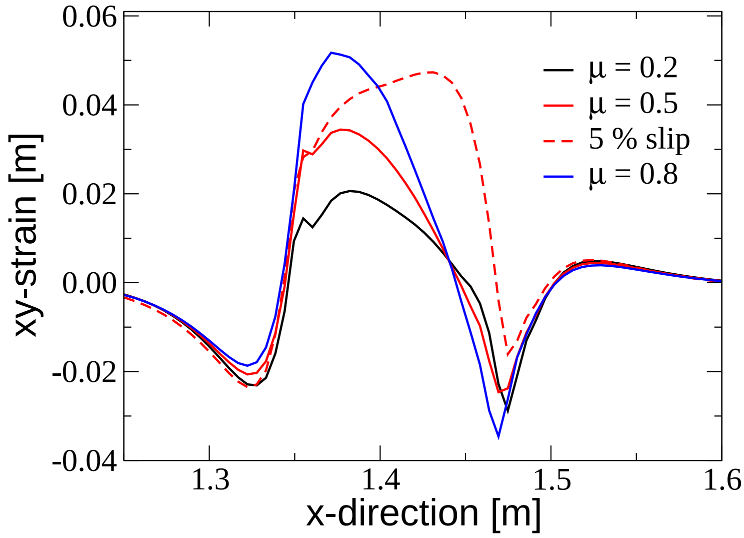

b)

Fig. 9. Stress in x-direction **a)** and xy-strain **b)** at the 3D-model. The sensor was assumed to be located inside of the tread. The curves are calculated without slip for different road conditions and with a slip of 5 % for a μ-value of 0.5.